Supplementary Information for Prediction of Threonine-Tyrosine Kinase Receptor-Ligand Unbinding Kinetics with Multiscale Milestoning and Metadynamics

Lane W. Votapka[1], Anupam Anand Ojha[1,2], Naoya Asada[3], and Rommie E. Amaro[4,*]

1 Department of Chemistry and Biochemistry, University of California San Diego, La Jolla, CA 92093, USA

2 Center for Computational Biology and Center for Computational Mathematics, Flatiron Institute, NY 10010, USA

3 Laboratory for Medicinal Chemistry Research, Shionogi & CO. Ltd, Osaka 541-0045, Japan.

4 Department of Molecular Biology, University of California San Diego, La Jolla, CA 92093, USA

* Email: ramaro@ucsd.edu

Computational Methods

All SEEKR calculations were performed using the crystal structures 5LJJ[1], 5N84[2], 5N93[2], 5N7V[2], 5NAD[2], 2X9E[3], 3GFW[4], and 3H9F[4]. For the preparation, the protein preparation wizard in Schrödinger 2021 suite[5] was used to add hydrogen atoms and consider the protonation state of the system. Protonation states of TTK were initially found with the Schrodinger Epik program within Maestro and later confirmed and adjusted using PDB2PQR[6]. TTK experimental kinetics and thermodynamics values were obtained from a study that recognized the importance of residence time to the cellular potency of the TTK target[2]. The protein and solvent portions of the system were parameterized using the LEAP program within the AmberTools 20[7] software suite. We created the topologies and initial coordinate files using the Amber ff19SB force field[8] for the protein with the GAFF force field[9] and AM1BCC charge were assigned for the ligand, though then reassigned with QMrebind[10] following energy minimization. TIP4P-Ew model was employed for water parameters[11]. Within QMrebind, the protein-ligand complexes were partitioned into three regions: the high-level QM region, comprised of the ligand itself; the low-level QM2 region, comprised of complete residues with any atoms residing within 5 Å of any of the ligand atoms, and finally, the MM region, which contained all the rest of the atoms. The QM region was modeled using the cc-pVTZ basis set with an MP2 method for the inner QM region. The QM2 region was modeled with the GFN2-XTB semiempirical tight-binding method[12]. Structures were then minimized and equilibrated using OpenMM[13]. CPPtraj was used to auto-image the solvent around the complex[14].

All systems contained a site center-of-mass to ligand center-of-mass (COM-COM) distance CV. Unless specified otherwise, all active sites atom definitions (to characterize the COM-COM distance CV) were defined by examining the native bound structure, selecting all alpha carbon atoms within 3 Å of the COM of the ligand, and then gradually removing them one

at a time, or adding more alpha carbons within 6 Å of the COM of the ligand, until the set of alpha carbons defining the site had a COM within 0.5 Å of the ligand COM. Following this, milestone spacings were chosen in a system-dependent manner, typically choosing closer spacings for regions of the CV where the ligand is within the site and wider spacings for CV regions where the ligand is out of the site or immersed in the solvent. Details on CV definitions and milestoning placements for each system are provided in the supplementary information tables S4 and S5. Following parameterization and equilibration, SMD simulations were run within HIDR of SeekrTools for 1μs for all systems with a restraint force constant of $9 \cdot 10^4$ kJ/(mol·nm^2) , and starting structures were saved every time the anchor point was crossed. MetaD simulations were run within HIDR with a Gaussian width of 0.05 nm, a Gaussian height of 1.0 kJ/mol, a bias factor of 10, and a deposition interval of 250 timesteps. MetaD parameters, such as Gaussian heights, widths, bias factors, and deposition intervals were chosen by performing a literature review on several similar applications of metaD,[15–18] and choosing characteristic values for each of them, and then refined based on visual assessment of the quality of generated starting structures, and their ability to generate accurate results with SEEKR. Binding site definitions for the TTK system can be found in Table S4.

Milestone placements for system TTK can be found in Table S5. The system structures were saved upon the last time that the simulations crossed each anchor point along the relevant CV. Although the metaD Gaussian height parameter was system-dependent, all metaD simulations used a sigma value of 1.0 Å and a bias factor of 10. Following this, SEEKR2 runs were performed in parallel for 500 ns per anchor using MMVT milestoning, which uses OpenMM as its MD engine[13], and all systems were subsequently analyzed using the native SEEKR2 and SeekrTools analysis programs. PQR files were prepared directly from AMBER parameter/topology files output from LEAP, using the MM partial charges and the radii from the mbondi2 set for the atomic charges and radii, respectively. The Browndye programs were used to prepare and run all BD simulations within the SEEKR framework[19]. Biomolecular images were generated with VMD[20].

The mean absolute error (MAE) for any set of data was computed with: $\sum_i \left| x_{i,calc} - x_{i,exp} \right|$ where $x_{i,calc}$ and $x_{i,exp}$ are the SEEKR-calculated and experimental quantities, respectively, that are being compared. In some cases, differences between calculated and experimental quantities exceeded many orders of magnitude, so the logarithm base ten of the calculated and experimental data, $log_{10}(x_{i,calc})$ and $log_{10}(x_{i,exp})$ were used to obtain the mean absolute $\log_{10}$ error. The ΔG_{bind} values computed from the relative free energies of MMVT anchors were found using the equation $k_B T \cdot \ln(\pi_{escaped}/\pi_{bound})$, where π_α is the stationary probability of anchor α, and is found using MMVT theory[21].

Benchmarking and Simulation Costs

We chose to simulate each anchor for 500 ns, and since each system possessed 23 simulated anchors, each different system required 11,500 ns - a total of 184,000 ns required for the MMVT simulations of all sixteen systems. The SMD simulations were run for 1000 ns per system, requiring a total of 8000 ns MD for the eight SMD systems (metaD simulations were relatively short - in the tens of ns - so we neglected these simulation costs). The anchors were

benchmarked to run at approximately 315 ns/day on a V100 GPU. Since all anchors for a system could be run synchronously on a large GPU cluster, the entire SEEKR2 calculation for a system (using metaD) could be completed in approximately 40 hours, using ~875 GPU hours per metaD system. To run SMD required an additional 1000 ns per system, which needed approximately 76 additional hours, for a final cost of ~950 GPU hours for SMD SEEKR2 calculations. The eight metaD systems and eight SMD systems, therefore, required approximately 15,330 GPU hours to complete.

All SEEKR-derived results within cells of Table S1 and S2 are highlighted by color according to their closeness to experimental values. For k_{on} and k_{off}, green indicates a SEEKR result within a single order of magnitude difference from the experiment, yellow indices within two orders of magnitude, orange within three orders of magnitude, and red is a SEEKR result that deviates more than three orders of magnitude from the experimental value. For ΔG_{bind} , green indicates a SEEKR result within one kcal/mol of difference from the experiment, yellow indices within two kcal/mol, orange within three kcal/mol, and red is a SEEKR result that deviates more than three kcal/mol from the experimental value.

Table S1 - Unbinding kinetics for TTK systems

TTK System (PDB ID)	Experimental k_{off} (s^{-1})	SEEKR k_{off} (s^{-1}) using 1000 ns SMD, with QMrebind	SEEKR k_{off} (s^{-1}) using MetaD, with QMrebind (correct protonation)
Reversine (5LJJ)	$1.00 \cdot 10^{-4}$	$(3.1 \pm 0.2) \cdot 10^{8}$	$(2.03 \pm 0.09) \cdot 10^{-5}$
MPI-0479605 (5N7V)	$3.40 \cdot 10^{-3}$	$(2.26 \pm 0.08) \cdot 10^{-6}$	$(1.46 \pm 0.08) \cdot 10^{-3}$
TC-Mps1-12 (5N93)	$4.70 \cdot 10^{-2}$	$(5.70 \pm 0.05) \cdot 10^{-2}$	$(8.99 \pm 0.06) \cdot 10^{-2}$
BAY 1217389 (5NAD)	$4.10 \cdot 10^{-4}$	$(9.2 \pm 0.1) \cdot 10^{-4}$	$(2.01 \pm 0.03) \cdot 10^{-3}$
Mps-BAY2b (5N84)	$2.80 \cdot 10^{-2}$	$(1.30 \pm 0.02) \cdot 10^{-6}$	$(8.3 \pm 0.2) \cdot 10^{-1}$
NMS-P715 (2X9E)	$8.33 \cdot 10^{-4}$	$(7.1 \pm 0.3) \cdot 10^{-11}$	$(2.29 \pm 0.02) \cdot 10^{-3}$
Mps1-IN-1 (3GFW)	$8.33 \cdot 10^{-3}$	$(3.7 \pm 0.1) \cdot 10^{-8}$	$(1.36 \pm 0.02) \cdot 10^{1}$
Mps1-IN-2 (3H9F)	$5.0 \cdot 10^{-2}$	$(6.6 \pm 1.8) \cdot 10^{-1}$	$(2.00 \pm 0.09) \cdot 10^{1}$

Table S2 - Binding kinetics and free energies for TTK systems

Compound	Experimental k_{on} (1/s·M)	SEEKR k_{on} (1/s·M)	Experimental ΔG_{bind} (kcal/mol)	SEEKR ΔG_{bind} from K_D (kcal/mol)	SEEKR ΔG_{bind} from milestoning (kcal/mol)
Reversine (5LJJ)	$2.08 \cdot 10^6$	$(2.8 \pm 0.1) \cdot 10^6$	14.0	15.18 ± 0.04	17.54 ± 0.03
MPI-0479605 (5N7V)	$1.96 \cdot 10^6$	$(9. \pm 1.) \cdot 10^5$	12.0	12.00 ± 0.07	15.34 ± 0.07
TC-Mps1-12 (5N93)	$2.16 \cdot 10^7$	$(3.4 \pm 0.4) \cdot 10^4$	11.8	7.61 ± 0.06	14.033 ± 0.003
BAY 1217389 (5NAD)	$3.79 \cdot 10^5$	$(2.5 \pm 0.2) \cdot 10^6$	12.2	12.41 ± 0.04	16.01 ± 0.02
Mps-BAY2b (5N84)	$2.60 \cdot 10^6$	$(1.69 \pm 0.09) \cdot 10^6$	10.9	8.60 ± 0.04	12.31 ± 0.08
NMS-P715 (2X9E)	$6.41 \cdot 10^5$	$(2.3 \pm 0.2) \cdot 10^5$	12.1	10.95 ± 0.04	14.67 ± 0.05
Mps1-IN-1 (3GFW)	$3.79 \cdot 10^5$	$(1.17 \pm 0.06) \cdot 10^6$	10.4	6.79 ± 0.03	9.764 ± 0.006
Mps1-IN-2 (3H9F)	$1.19 \cdot 10^6$	$(9.4 \pm 0.4) \cdot 10^5$	10.4	8.20 ± 0.04	7.68 ± 0.03

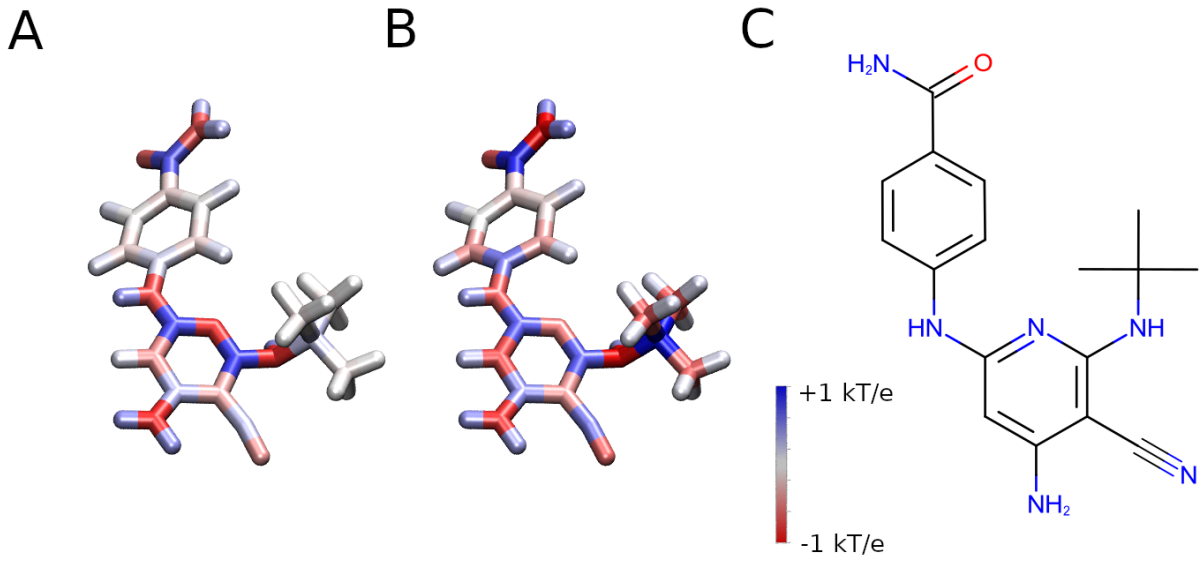

Figure S1 - Reparametrization of charges using QMrebind on compound TC-Mps1-12. (A) Charges of the compound assigned by ordinary AM1BCC in GAFF. (B) Charges on the same compound reparametrized with QMrebind - note the changes to the charges on the tert-butyl group. (C) 2D representation of the compound for reference.

Table S3 - TTK system ligand charge reparametrization from AM1BCC charges to QMrebind charges

All charges in units of proton charge

Reversine (5LJJ) charges				MPI-0479605 (5N7V) charges				TC-Mps1-12 (5N93) charges		
Atom Name	AM1BCC charge	QMrebind charge		Atom Name	AM1BCC charge	QMrebind charge		Atom Name	AM1BCC charge	QMrebind charge
C1	-0.0944	-0.5019		C6	-0.0939	-0.1837		C12	-0.1061	-0.6005
H1	0.049	0.129		H2	0.0542	0.0599		H7	0.0459	0.1131
H2	0.049	0.1117		H3	0.0542	0.072		H8	0.0459	0.1471
C2	-0.0749	0.1215		C7	-0.0814	-0.1837		H9	0.0459	0.1355
H3	0.0429	0.028		H4	0.041	0.0742		C11	0.2452	1.0591
H4	0.0429	-0.011		H5	0.041	0.0449		C13	-0.1061	-0.6519
C3	-0.0804	-0.1794		C8	-0.0794	0.0622		H10	0.0459	0.129
H5	0.0407	0.0728		H6	0.0407	0.0063		H11	0.0459	0.1412
H6	0.0407	0.0686		H7	0.0407	0.0047		H12	0.0459	0.1592
C4	-0.0749	-0.0702		C9	-0.0814	-0.0745		C14	-0.1061	-0.669
H7	0.0429	0.0434		H8	0.041	0.0158		H13	0.0459	0.1677
H8	0.0429	0.0572		H9	0.041	0.0289		H14	0.0459	0.1638
C5	-0.0944	-0.1845		C10	-0.0939	-0.1424		H15	0.0459	0.1442
H9	0.049	0.0245		H10	0.0542	0.0387		N3	-0.8519	-1.0205
H10	0.049	0.0595		H11	0.0542	0.0336		H6	0.4338	0.396
C6	0.2185	0.6276		C11	0.2115	0.5768		C7	0.7822	0.6644
H11	0.0837	-0.0157		H12	0.0917	-0.0061		N4	-0.813	-0.5276
N1	-0.8409	-0.6746		N1	-0.8249	-0.8405		C6	-0.3393	-0.4166
H12	0.4428	0.3065		H13	0.4238	0.3329		C8	0.2558	0.5165
C7	0.7802	0.358		C3	0.7712	0.6129		N1	-0.4088	-0.6085
C8	-0.2602	0.1889		N2	-0.823	-0.6151		C9	0.3206	0.4544
N3	-0.5341	-0.5931		C2	-0.2402	-0.0113		N2	-0.8592	-0.8209
C9	0.3907	0.1114		N3	-0.5341	-0.5477		H3	0.4318	0.4188
N4	-0.387	-0.4939		C4	0.3897	0.1152		H4	0.4318	0.3752
C10	0.4878	0.5836		N4	-0.389	-0.4469		C10	-0.4453	-0.7095
N5	-0.79	-0.9598		H14	0.3157	0.4094		H5	0.143	0.273
H14	0.3157	0.4028		H1	0.0708	0.185		C5	0.7442	0.6614
H13	0.0708	0.1757		C1	0.4838	0.628		N5	-0.7303	-0.6564
N2	-0.816	-0.6249		N5	-0.79	-0.9883		H16	0.4298	0.3847
C11	0.9159	0.8978		C5	0.9159	0.7459		C3	0.1716	0.5202
N6	-0.6983	-0.7445		N6	-0.6973	-0.3601		C2	-0.1615	-0.4007
H15	0.4328	0.439		H15	0.4318	0.3318		H1	0.1475	0.2142
C12	0.1026	0.449		C12	0.0976	-0.1646		C15	-0.073	-0.0297
C15	-0.111	-0.248		C16	-0.073	-0.1707		H17	0.146	0.1685

C16	-0.157	-0.4389		C17	-0.175	-0.4483		C1	-0.1636	-0.1788
H19	0.135	0.2334		H21	0.132	0.2414		C17	0.6737	0.8746
H18	0.1425	0.2023		H20	0.151	0.1887		O1	-0.6131	-0.656
C13	-0.111	-0.3334		C13	-0.0833	0.6771		N6	-0.675	-1.1166
H16	0.1425	0.2102		C14	-0.0608	-0.5909		H19	0.3115	0.4573
C14	-0.157	-0.1987		H16	0.047	0.1237		H20	0.3115	0.4752
H17	0.135	0.1539		H17	0.047	0.1947		C16	-0.073	-0.1384
C17	0.1236	0.2423		H18	0.047	0.0968		H18	0.146	0.1933
N7	-0.628	-0.3323		C15	-0.145	-0.7716		C4	-0.1615	-0.3634
C18	0.1478	0.2669		H19	0.137	0.2236		H2	0.1475	0.1573
H20	0.0474	-0.0087		C18	0.1266	0.5981				
H21	0.0474	-0.0447		N7	-0.622	-0.3619				
C19	0.1239	-0.0323		C19	0.1478	0.0271				
H22	0.0559	0.0937		H22	0.0597	0.0546				
H23	0.0559	0.0562		H23	0.0597	0.0259				
O1	-0.4146	-0.4248		C20	0.1029	0.2857				
C20	0.1239	-0.0378		H24	0.0519	0.0031				
H24	0.0559	0.1137		H25	0.0519	0.0016				
H25	0.0559	0.0806		O1	-0.4136	-0.5335				
C21	0.1478	0.1507		C21	0.1029	0.2136				
H26	0.0474	0.0612		H26	0.0519	0.0344				
H27	0.0474	0.0319		H27	0.0519	0.0572				
				C22	0.1478	-0.1933				
				H28	0.0597	0.1054				
				H29	0.0597	0.103				
BAY 1217389 (5NAD)				Mps-BAY2b (5N84)				NMS-P715 (2X9E)		
Atom Name	AM1BCC charge	QMrebind charge		Atom Name	AM1BCC charge	QMrebind charge		Atom Name	AM1BCC charge	QMrebind charge
F2	-0.1059	-0.1409		C19	-0.0926	-0.4492		C22	0.115	-0.194
C15	0.1409	0.0041		H18	0.0369	0.0772		C23	-0.131	-0.143
C9	0.0259	0.3167		H19	0.0369	0.0911		H23	0.090	0.121
F1	-0.1259	-0.1757		H20	0.0369	0.113		H24	0.090	0.145
C10	0.1251	-0.0224		C18	-0.1017	0.5717		H21	0.105	0.132
O2	-0.3209	-0.2711		C20	-0.0926	-0.7372		H22	0.105	0.138
C11	0.1107	-0.0816		H21	0.0369	0.1475		N8	-0.686	0.062
H7	0.054	0.0645		H22	0.0369	0.1404		C24	0.084	-0.528
H8	0.054	0.0453		H23	0.0369	0.1717		H25	0.106	0.211
H9	0.054	0.1462		H17	0.0637	-0.048		H26	0.106	0.245

C12	-0.146	-0.0819		C17	0.1988	-0.1145		H27	0.106	0.191
H10	0.165	0.1799		H15	0.0667	0.0821		H20	0.447	0.355
C13	-0.081	-0.4551		H16	0.0667	0.1163		C21	0.115	-0.297
H11	0.162	0.2402		N5	-0.8219	-0.4903		H18	0.105	0.170
C14	0.0401	0.4388		H14	0.4388	0.3555		H19	0.105	0.175
O1	-0.3414	-0.4088		C14	0.7132	0.5858		C20	-0.131	-0.071
C1	0.6406	0.7315		C15	-0.1936	0.0988		H16	0.090	0.132
N1	-0.5728	-0.688		N4	-0.2706	-0.6372		H17	0.090	0.094
C3	-0.3703	-0.5121		C16	0.0236	0.1169		C19	0.105	0.282
H1	0.171	0.2491		H13	0.186	0.1634		H15	0.108	0.076
C2	0.2936	-0.0211		N3	-0.742	-0.6065		N7	-0.586	-0.842
N4	-0.7486	-0.2909		C13	0.4082	0.2372		H14	0.319	0.395
C6	0.2088	-0.0277		H12	0.0371	0.142		C18	0.696	0.886
C7	-0.1374	-0.2293		C12	-0.2586	-0.789		O3	-0.593	-0.696
C8	0.6209	0.8003		H11	0.177	0.3257		C15	-0.200	-0.157
F3	-0.2386	-0.3084		N2	0.0737	0.7065		C16	-0.061	-0.235
F4	-0.2386	-0.2709		C11	-0.1283	-0.5371		C17	-0.171	-0.190
F5	-0.2386	-0.2616		C8	0.0102	0.565		H13	0.169	0.199
H5	0.0962	0.116		C9	-0.132	-0.4579		H12	0.131	0.153
H6	0.0962	0.0792		C10	-0.0875	0.0508		C14	-0.023	-0.297
H3	0.0827	0.1201		H10	0.1485	0.1112		H11	0.179	0.178
H4	0.0827	0.1074		H9	0.143	0.1795		C13	-0.001	0.385
H12	0.4378	0.3338		C7	-0.132	-0.4507		O2	-0.367	-0.408
C16	-0.1273	0.4219		H8	0.143	0.2363		C25	0.813	0.883
N3	-0.2706	-0.5404		C6	-0.0875	-0.0389		F1	-0.209	-0.218
C5	0.0046	-0.1139		H7	0.1485	0.1637		F2	-0.209	-0.201
H2	0.188	0.2245		C5	-0.1416	-0.2261		F3	-0.209	-0.284
N2	0.2302	0.4146		C1	0.6777	0.7165		C12	0.251	0.198
C4	-0.0693	-0.3496		O1	-0.5981	-0.6415		N6	-0.727	-0.628
C17	0.0042	0.6003		N1	-0.5419	-0.6215		H10	0.480	0.423
C23	-0.109	-0.5479		H1	0.3115	0.3135		C11	0.872	0.962
C21	-0.0253	0.3668		C2	0.0537	0.2501		N5	-0.747	-0.702
C22	-0.0718	-0.6059		H2	0.1227	0.0823		C8	0.554	0.556
H15	0.058	0.1979		C3	-0.1539	-0.1529		N4	-0.710	-0.822
H16	0.058	0.1978		H3	0.0739	0.1093		C10	0.461	0.384
H17	0.058	0.1645		H4	0.0739	0.1436		H9	0.044	0.127
H18	0.152	0.2505		C4	-0.1539	-0.5603		C9	-0.308	-0.346
C18	-0.127	-0.4662		H5	0.0739	0.2		C2	-0.025	-0.152
H13	0.14	0.1788		H6	0.0739	0.1942		H3	0.065	0.098

C19	-0.105	-0.0977						H4	0.065	0.099
H14	0.14	0.2002						C1	-0.016	-0.002
C20	-0.1396	-0.3167						H1	0.085	0.042
C24	0.6817	0.9213						H2	0.085	0.081
O3	-0.5971	-0.7766						C3	-0.134	0.045
N5	-0.5439	-0.623						C4	-0.220	-0.228
H19	0.3135	0.3949						N1	0.147	0.347
C25	0.0537	0.0554						C7	0.040	-0.295
H20	0.1217	0.1797						H6	0.067	0.105
C26	-0.1544	-0.4717						H7	0.067	0.158
H21	0.0737	0.1776						H8	0.067	0.111
H22	0.0737	0.1806						N2	-0.486	-0.478
C27	-0.1544	-0.1481						C5	0.252	-0.023
H23	0.0737	0.0965						C6	0.601	0.797
H24	0.0737	0.1083						O1	-0.588	-0.697
								N3	-0.462	-0.415
								H5	0.324	0.322
								C26	0.024	-0.136
								C27	-0.064	0.282
								C34	-0.043	-0.149
								C35	-0.093	-0.155
								H38	0.037	0.052
								H39	0.037	0.024
								H40	0.037	0.018
								H36	0.054	0.099
								H37	0.054	0.083
								C28	-0.128	-0.403
								H28	0.139	0.189
								C29	-0.123	0.094
								H29	0.135	0.151
								C30	-0.128	-0.687
								H30	0.139	0.306
								C31	-0.064	0.189
								C32	-0.043	0.137
								H31	0.054	0.001
								H32	0.054	0.063
								C33	-0.093	-0.334
								H33	0.037	0.076
								H34	0.037	0.110

								H35	0.037	0.076
Mps1-IN-1 (3GFW)				Mps1-IN-2 (3H9F)						
Atom Name	AM1BCC charge	QMrebind charge		Atom Name	AM1BCC charge	QMrebind charge				
C1	0.197	-0.208		C4	0.198	0.084				
H1	0.044	0.161		H2	0.046	0.094				
H2	0.044	0.030		H3	0.046	0.065				
C2	-0.125	0.131		C5	-0.109	-0.413				
H3	0.062	-0.037		H4	0.062	0.128				
H4	0.062	0.000		H5	0.062	0.139				
C3	0.142	0.291		C6	0.144	0.490				
O1	-0.596	-0.676		O1	-0.601	-0.763				
H6	0.399	0.369		H7	0.400	0.376				
H5	0.078	-0.054		H6	0.036	-0.026				
C4	-0.125	-0.063		C7	-0.109	-0.051				
H7	0.062	0.005		H8	0.062	-0.038				
H8	0.062	0.022		H9	0.062	0.060				
C5	0.197	0.043		C8	0.198	0.034				
H9	0.044	0.000		H10	0.046	-0.007				
H10	0.044	0.080		H11	0.046	0.088				
N1	-0.654	-0.032		N3	-0.651	-0.272				
C6	0.191	0.080		C9	0.185	0.203				
C10	-0.220	-0.411		C13	-0.217	-0.399				
C11	-0.059	-0.202		C14	-0.045	-0.108				
H16	0.150	0.200		H17	0.154	0.185				
H15	0.138	0.258		H16	0.138	0.206				
C7	-0.246	-0.273		C10	-0.240	-0.355				
H11	0.143	0.116		H12	0.142	0.143				
C8	0.134	0.289		C11	0.128	0.285				
O2	-0.333	-0.342		O2	-0.341	-0.370				
C9	0.116	-0.026		C12	0.118	0.059				
H12	0.047	0.011		H13	0.046	0.078				
H13	0.047	0.097		H14	0.046	0.099				
H14	0.047	0.109		H15	0.046	-0.004				
C12	0.032	0.153		C15	0.050	0.055				
N2	-0.684	-0.558		N4	-0.668	-0.536				
H17	0.425	0.368		H18	0.439	0.362				
C13	0.669	0.841		C16	0.866	0.847				

N3	-0.743	-1.023		N2	-0.766	-0.551				
C15	0.481	0.820		N1	-0.737	-0.877				
N4	-0.294	-0.561		C3	0.450	0.434				
C16	-0.116	-0.114		H1	0.034	0.130				
C17	-0.163	-0.417		C2	-0.235	-0.289				
C18	-0.268	-0.256		C1	0.662	0.458				
H21	0.166	0.210		N6	-0.738	-0.373				
H20	0.169	0.209		C21	0.206	0.358				
H19	0.309	0.450		C22	-0.093	-0.123				
C14	-0.340	-0.821		C23	-0.080	-0.043				
H18	0.156	0.262		C24	-0.080	-0.061				
C19	0.245	0.558		C25	-0.093	-0.069				
N5	-0.653	-0.641		H33	0.051	0.039				
H22	0.480	0.425		H34	0.051	0.012				
C20	0.315	0.351		H31	0.042	0.012				
C21	-0.218	-0.244		H32	0.042	0.056				
H23	0.158	0.155		H29	0.042	-0.002				
C22	-0.032	-0.122		H30	0.042	0.069				
H24	0.135	0.176		H27	0.051	0.019				
C23	-0.199	-0.238		H28	0.051	-0.003				
H25	0.142	0.164		H26	0.073	-0.003				
C24	-0.006	-0.090		C20	0.193	0.017				
H26	0.157	0.175		H24	0.052	0.030				
C25	-0.460	-0.157		H25	0.052	0.153				
S1	1.366	0.969		C19	-0.159	-0.392				
O3	-0.663	-0.566		H22	0.080	0.165				
O4	-0.663	-0.632		H23	0.080	0.106				
C26	-0.261	0.239		C18	0.714	0.822				
C28	-0.071	-0.633		O3	-0.636	-0.764				
H31	0.049	0.206		N5	-0.363	-0.206				
H32	0.049	0.147		C17	0.082	-0.342				
H33	0.049	0.177		H19	0.049	0.160				
H27	0.113	0.132		H20	0.049	0.175				
C27	-0.071	-0.510		H21	0.049	0.148				
H28	0.049	0.150								
H29	0.049	0.106								
H30	0.049	0.176								

Figure S2 - Convergence of k_{off} for TTK Systems

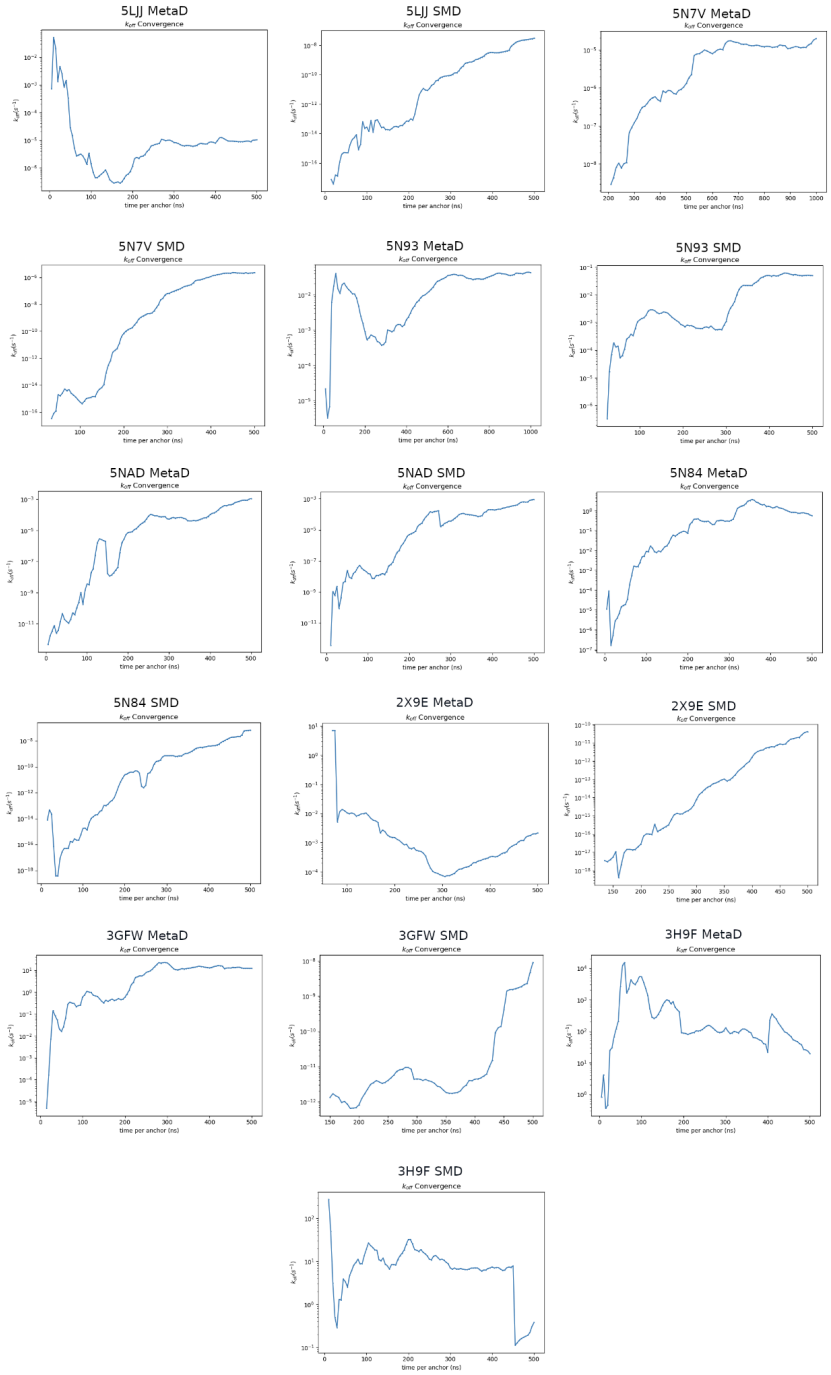

Figure S2: Convergence of k_{off} values for TTK systems. Typically, we may assume that a system is converged if the k_{off} fluctuates within only an order of magnitude during the last half of the simulation. Using these criteria, many SMD simulations are not fully converged within the 1000ns of the SEEKR simulations, with the possible exception of 5NAD SMD. While MetaD simulations were more likely to converge (probably due to more energetically-favorable chosen starting structures), not all were converged by the end of the simulation - 5N84, for instance.

Table S4 - TTK system binding site definitions

Sites were chosen by selecting alpha carbons (Cα) of all residues with any atoms within 0.3 nm of any atoms of the ligand, then individually adding nearby residue Cαs or removing residue Cαs from the selection until the center of mass (COM) of the site fell within 0.05 nm of the ligand COM.

Ligand (PDBID)	Site Atoms (Atom Name - Residue Name - Residue Index)
Reversine (5LJJ)	CA-ILE-531, CA-VAL-539, CA-ALA-551, CA-TYR-604, CA-GLY-605, CA-ILE-607, CA-ASP-608, CA-ALA-651, CA-LEU-654, CA-ILE-663, CA-THR-675
MPI-0479605 (5N7V)	CA-VAL-539, CA-GLN-541, CA-ALA-551, CA-CYS-604, CA-ILE-607, CA-ASP-608, CA-LEU-654, CA-ILE-663, CA-MET-671
TC-Mps1-12 (5N93)	CA-VAL-539, CA-GLN-541, CA-ALA-551, CA-CYS-604, CA-ILE-607, CA-ASP-608, CA-LEU-654, CA-ILE-663, CA-MET-671
BAY 1217389 (5NAD)	CA-LYS-529, CA-ILE-531, CA-GLN-541, CA-ALA-551, CA-LYS-553, CA-ILE-586, CA-MET-602, CA-CYS-604, CA-GLY-605, CA-ASP-608, CA-LYS-649, CA-ALA-651, CA-LEU-654, CA-ILE-663, CA-MET-671, CA-PRO-673
Mps-BAY2b (5N84)	CA-ILE-531, CA-VAL-539, CA-LYS-553, CA-LEU-575, CA-CYS-604, CA-ILE-607, CA-ASP-608, CA-ILE-663, CA-VAL-684
NMS-P715 (2X9E)	CA-LEU-528, CA-LYS-529, CA-GLN-530, CA-ILE-531, CA-GLY-532, CA-SER-533, CA-GLY-534, CA-SER-537, CA-LYS-538, CA-VAL-539, CA-GLN-541, CA-ALA-551, CA-LYS-553, CA-MET-602, CA-GLU-603, CA-CYS-604, CA-GLY-605, CA-ASN-606, CA-ILE-607, CA-ASP-608, CA-SER-611, CA-TRP-612, CA-LYS-614, CA-LYS-615, CA-ALA-651, CA-ASN-652, CA-LEU-654, CA-ILE-663
Mps1-IN-1 (3GFW)	CA-LYS-529, CA-ILE-531, CA-GLY-532, CA-SER-533, CA-SER-537, CA-VAL-539, CA-GLN-541, CA-ALA-551, CA-LYS-553, CA-ILE-586, CA-GLU-603, CA-CYS-604, CA-GLY-605, CA-ASN-606, CA-ILE-607, CA-ASP-608, CA-SER-611, CA-LYS-614, CA-LYS-615, CA-ALA-651, CA-ASN-652, CA-LEU-654, CA-PRO-673, CA-THR-676
Mps1-IN-2 (3H9F)	CA-ILE-531, CA-LYS-553, CA-MET-602, CA-CYS-604, CA-GLY-605, CA-ILE-607, CA-SER-611, CA-LEU-654, CA-PRO-673, CA-TPO-675

Table S5 - TTK system anchor radii

For the BAY 1217389 and Mps-BAY2b systems, because of the large size of those ligands, a set of anchors that ended at a further distance from the site was observed to better represent the unbound state. The radii highlighted in **bold** show the state that was considered "escaped" for k_{off} calculations (chosen by visual inspection of SEEKR trajectories - the distance when the ligand could traverse to regions of the protein surface other than the immediate opening of the binding site). The higher anchors were still used for k_{on} calculations.

Ligand (PDBID)	**Anchor radii (nm)**
Reversine (5LJJ)	0.1500, 0.2250, 0.3000, 0.3750, 0.4500, 0.5250, 0.6000, 0.6750, 0.7750, 0.8750, 1.0000, 1.1000, 1.2000, 1.3000, 1.4000, 1.5000, 1.6000, 1.7000, 1.8000, **1.9000,** 2.0000, 2.2000, 2.4000, 2.6000
MPI-0479605 (5N7V)	0.1500, 0.2250, 0.3000, 0.3750, 0.4500, 0.5250, 0.6000, 0.7000, 0.8000, 0.9000, 1.0000, 1.1000, 1.2000, 1.3000, 1.4000, 1.5000, 1.6000, 1.7000, 1.8000, **1.9000,** 2.0000, 2.2000, 2.4000, 2.6000
TC-Mps1-12 (5N93)	0.1500, 0.2250, 0.3000, 0.3750, 0.4500, 0.5250, 0.6000, 0.7000, 0.8000, 0.9000, 1.0000, 1.1000, 1.2000, 1.3000, 1.4000, 1.5000, **1.6000**, 1.7000, 1.8000, 1.9000**,** 2.0000, 2.2000, 2.4000, 2.6000
BAY 1217389 (5NAD)	0.1500, 0.2250, 0.3000, 0.3750, 0.4500, 0.5250, 0.6000, 0.7000, 0.8000, 0.9000, 1.0000, 1.1000, 1.2000, 1.3000, 1.4000, 1.5000, 1.6000, 1.7000, 1.8000, 2.0000, 2.2000, 2.4000, **2.6000**, 2.8000
Mps-BAY2b (5N84)	0.1500, 0.2250, 0.3000, 0.3750, 0.4500, 0.5250, 0.6000, 0.7000, 0.8000, 0.9000, 1.0000, 1.1000, 1.2000, 1.3000, 1.4000, 1.5000, 1.6000, 1.7000, **1.8000**, 2.0000, 2.2000, 2.4000, 2.6000, 2.8000
NMS-P715 (2X9E)	0.1500, 0.2250, 0.3000, 0.3750, 0.4500, 0.5250, 0.6000, 0.7000, 0.8000, 0.9000, 1.0000, 1.1000, 1.2000, 1.3000, 1.4000, 1.5000, 1.6000, 1.7000, 1.8000, 2.0000, 2.2000, 2.4000, **2.6000**, 2.8000
Mps1-IN-1 (3GFW)	0.1500, 0.2250, 0.3000, 0.3750, 0.4500, 0.5250, 0.6000, 0.7000, 0.8000, 0.9000, 1.0000, 1.1000, 1.2000, 1.3000, 1.4000, 1.5000, 1.6000, 1.7000, 1.8000, 2.0000, 2.2000, 2.4000, **2.6000**, 2.8000
Mps1-IN-2 (3H9F)	0.1500, 0.2250, 0.3000, 0.3750, 0.4500, 0.5250, 0.6000, 0.7000, 0.8000, 0.9000, 1.0000, 1.1000, 1.2000, 1.3000, 1.4000, 1.5000, 1.6000, 1.7000, 1.8000, 2.0000, 2.2000, 2.4000, **2.6000**, 2.8000

References

(1) Hiruma, Y.; Koch, A.; Dharadhar, S.; Joosten, R. P.; Perrakis, A. Structural Basis of Reversine Selectivity in Inhibiting Mps1 More Potently than Aurora B Kinase. *Proteins Struct. Funct. Bioinforma.* **2016**, *84* (12), 1761–1766. https://doi.org/10.1002/prot.25174.

(2) Uitdehaag, J. C. M.; de Man, J.; Willemsen-Seegers, N.; Prinsen, M. B. W.; Libouban, M. A. A.; Sterrenburg, J. G.; de Wit, J. J. P.; de Vetter, J. R. F.; de Roos, J. A. D. M.; Buijsman, R. C.; Zaman, G. J. R. Target Residence Time-Guided Optimization on TTK Kinase Results in Inhibitors with Potent Anti-Proliferative Activity. *J. Mol. Biol.* **2017**, *429* (14), 2211–2230. https://doi.org/10.1016/j.jmb.2017.05.014.

(3) Colombo, R.; Caldarelli, M.; Mennecozzi, M.; Giorgini, M. L.; Sola, F.; Cappella, P.; Perrera, C.; Depaolini, S. R.; Rusconi, L.; Cucchi, U.; Avanzi, N.; Bertrand, J. A.; Bossi, R. T.; Pesenti, E.; Galvani, A.; Isacchi, A.; Colotta, F.; Donati, D.; Moll, J. Targeting the Mitotic Checkpoint for Cancer Therapy with NMS-P715, an Inhibitor of MPS1 Kinase. *Cancer Res.* **2010**, *70* (24), 10255–10264. https://doi.org/10.1158/0008-5472.CAN-10-2101.

(4) Kwiatkowski, N.; Jelluma, N.; Filippakopoulos, P.; Soundararajan, M.; Manak, M. S.; Kwon, M.; Choi, H. G.; Sim, T.; Deveraux, Q. L.; Rottmann, S.; Pellman, D.; Shah, J. V.; Kops, G. J. P. L.; Knapp, S.; Gray, N. S. Small-Molecule Kinase Inhibitors Provide Insight into Mps1 Cell Cycle Function. *Nat. Chem. Biol.* **2010**, *6* (5), 359–368. https://doi.org/10.1038/nchembio.345.

(5) Schrodinger Release 2021.

(6) Unni, S.; Huang, Y.; Hanson, R. M.; Tobias, M.; Krishnan, S.; Li, W. W.; Nielsen, J. E.; Baker, N. A. Web Servers and Services for Electrostatics Calculations with APBS and PDB2PQR. *J. Comput. Chem.* **2011**, *32* (7), 1488–1491. https://doi.org/10.1002/jcc.21720.

(7) Case, D. A.; Aktulga, H. M.; Belfon, K.; Cerutti, D. S.; Cisneros, G. A.; Cruzeiro, V. W. D.; Forouzesh, N.; Giese, T. J.; Götz, A. W.; Gohlke, H.; Izadi, S.; Kasavajhala, K.; Kaymak, M. C.; King, E.; Kurtzman, T.; Lee, T.-S.; Li, P.; Liu, J.; Luchko, T.; Luo, R.; Manathunga, M.; Machado, M. R.; Nguyen, H. M.; O'Hearn, K. A.; Onufriev, A. V.; Pan, F.; Pantano, S.; Qi, R.; Rahnamoun, A.; Risheh, A.; Schott-Verdugo, S.; Shajan, A.; Swails, J.; Wang, J.; Wei, H.; Wu, X.; Wu, Y.; Zhang, S.; Zhao, S.; Zhu, Q.; Cheatham, T. E. I.; Roe, D. R.; Roitberg, A.; Simmerling, C.; York, D. M.; Nagan, M. C.; Merz, K. M. Jr. AmberTools. *J. Chem. Inf. Model.* **2023**, *63* (20), 6183–6191. https://doi.org/10.1021/acs.jcim.3c01153.

(8) Tian, C.; Kasavajhala, K.; Belfon, K. A. A.; Raguette, L.; Huang, H.; Migues, A. N.; Bickel, J.; Wang, Y.; Pincay, J.; Wu, Q.; Simmerling, C. ff19SB: Amino-Acid-Specific Protein Backbone Parameters Trained against Quantum Mechanics Energy Surfaces in Solution. *J. Chem. Theory Comput.* **2020**, *16* (1), 528–552. https://doi.org/10.1021/acs.jctc.9b00591.

(9) Wang, J.; Wolf, R. M.; Caldwell, J. W.; Kollman, P. A.; Case, D. A. Development and Testing of a General Amber Force Field. *J. Comput. Chem.* **2004**, *25* (9), 1157–1174. https://doi.org/10.1002/jcc.20035.

(10) Ojha, A. A.; Votapka, L. W.; Amaro, R. E. QMrebind: Incorporating Quantum Mechanical Force Field Reparameterization at the Ligand Binding Site for Improved Drug-Target Kinetics through Milestoning Simulations. *ChemRxiv* **2023**.

(11) Horn, H. W.; Swope, W. C.; Pitera, J. W.; Madura, J. D.; Dick, T. J.; Hura, G. L.; Head-Gordon, T. Development of an Improved Four-Site Water Model for Biomolecular Simulations: TIP4P-Ew. *J. Chem. Phys.* **2004**, *120* (20), 9665–9678. https://doi.org/10.1063/1.1683075.

(12) Bannwarth, C.; Ehlert, S.; Grimme, S. GFN2-xTB—An Accurate and Broadly Parametrized Self-Consistent Tight-Binding Quantum Chemical Method with Multipole Electrostatics and Density-Dependent Dispersion Contributions. *J. Chem. Theory Comput.* **2019**, *15* (3), 1652–1671. https://doi.org/10.1021/acs.jctc.8b01176.

(13) Eastman, P.; Swails, J.; Chodera, J. D.; McGibbon, R. T.; Zhao, Y.; Beauchamp, K. A.; Wang, L. P.; Simmonett, A. C.; Harrigan, M. P.; Stern, C. D.; Wiewiora, R. P.; Brooks, B. R.;

Pande, V. S. OpenMM 7: Rapid Development of High Performance Algorithms for Molecular Dynamics. *PLoS Comput. Biol.* **2017**, *13* (7). https://doi.org/10.1371/journal.pcbi.1005659.
(14) Roe, D. R.; Cheatham, T. E. I. PTRAJ and CPPTRAJ: Software for Processing and Analysis of Molecular Dynamics Trajectory Data. *J. Chem. Theory Comput.* **2013**, *9* (7), 3084–3095. https://doi.org/10.1021/ct400341p.
(15) Ghosh, S.; Jana, K.; Ganguly, B. Revealing the Mechanistic Pathway of Cholinergic Inhibition of Alzheimer's Disease by Donepezil: A Metadynamics Simulation Study. *Phys. Chem. Chem. Phys.* **2019**, *21* (25), 13578–13589. https://doi.org/10.1039/C9CP02613D.
(16) Brandt, A. A. M. L.; Rodrigues-da-Silva, R. N.; Lima-Junior, J. C.; Alves, C. R.; de Souza-Silva, F. Combining Well-Tempered Metadynamics Simulation and SPR Assays to Characterize the Binding Mechanism of the Universal T-Lymphocyte Tetanus Toxin Epitope TT830-843. *BioMed Res. Int.* **2021**, *2021* (1), 5568980. https://doi.org/10.1155/2021/5568980.
(17) Wakchaure, P. D.; Ganguly, B. Deciphering the Mechanism of Action of 5FDQD and the Design of New Neutral Analogues for the FMN Riboswitch: A Well-Tempered Metadynamics Simulation Study. *Phys. Chem. Chem. Phys.* **2022**, *24* (2), 817–828. https://doi.org/10.1039/D1CP01348C.
(18) Zhou, X.; Shi, M.; Wang, X.; Xu, D. Exploring the Binding Mechanism of a Supramolecular Tweezer CLR01 to 14-3-3σ Protein via Well-Tempered Metadynamics. *Front. Chem.* **2022**, *10*. https://doi.org/10.3389/fchem.2022.921695.
(19) Huber, G. A.; McCammon, J. A. Browndye: A Software Package for Brownian Dynamics. *Comput. Phys. Commun.* **2010**, *181* (11). https://doi.org/10.1016/j.cpc.2010.07.022.
(20) Humphrey, W.; Dalke, A.; Schulten, K. VMD: Visual Molecular Dynamics. *J. Mol. Graph.* **1996**, *14* (1), 33–38. https://doi.org/10.1016/0263-7855(96)00018-5.
(21) Vanden-Eijnden, E.; Venturoli, M. Markovian Milestoning with Voronoi Tessellations. *J. Chem. Phys.* **2009**, *130* (19). https://doi.org/10.1063/1.3129843.